

To understand the roles of infall and protostellar evolution on the envelopes of massive young stellar objects (YSOs). The chemical evolution of gas and dust is traced, including infall and realistic source evolution. The temperatures are determined self-consistently. Both ad/desorption of ices using recent laboratory temperature-programmed-desorption measurements are included. The observed water abundance jump near 100 K is reproduced by an evaporation front which moves outward as the luminosity increases. Ion-molecule reactions produce water below 100 K. The age of the source is constrained to $t \sim 8 \pm 4 \times 10^4$ yrs since YSO formation. It is shown that the chemical age-dating of hot cores at \sim few $\times 10^3 - 10^4$ yr and the disappearance of hot cores on a timescale of $\sim 10^5$ yr is a natural consequence of infall in a dynamic envelope and protostellar evolution. Dynamical structures of ~ 350 AU such as disks should contain most of the complex second generation species. The assumed order of desorption kinetics does not affect these results.

Key words. stars: formation – stars: individual: AFGL 2591 – ISM: molecules – molecular processes

Astrochemical confirmation of the rapid evolution of massive YSOs and explanation for the inferred ages of hot cores

S. D. Doty,¹ E. F. van Dishoeck,² and J. C. Tan³

¹ Department of Physics and Astronomy, Denison University, Granville, OH, 43023, USA

² Sterrewacht Leiden, PO Box 9513, 2300 RA Leiden, The Netherlands

³ Department of Astronomy, University of Florida, P. O. Box 112055, Gainesville, FL, 32611, USA

Received ; accepted

Abstract.

1. Introduction

The physical and chemical structure of massive young stellar objects (YSOs) has been an area of increasing study (e.g. Beuther et al. 2006). While a wealth of new data and models have become available, many basic open questions remain. For example, the processes and timescales involved in the formation and evolution of the high-mass protostellar objects and ensuing “hot core” phase are not on firm theoretical ground.

Recently, McKee & Tan (2003) introduced the first realistic model for the evolution of massive YSOs, including a time-dependent accretion rate. By combining this with a model for the evolution of the protostar onto the ZAMS, they predicted the time-dependent total (source + accretion) luminosity for the lifetime of the massive YSO.

A test of the evolution is expected to be desorption of ices from grain mantles, as the evolving source heats the surrounding envelope. Laboratory data using temperature programmed desorption (TPD) have been recently reported (see e.g., Fraser et al. 2001). These data allow for a detailed analysis of the desorption of realistic ice mantles.

Models have included some, but not all, of these effects. While TPD data were included by Viti et al. (2004) and Lintott et al. (2005), these were single-point models and/or used approximate source evolution. Source evolution was considered by Rodgers & Charnley (2003) and Lee et al. (2004), but using low-mass YSO models. It is common to assume a static envelope, constant luminosity, and standard first-order desorption (e.g., Caselli et al. 1993; Nomura & Millar 2004). Viti & Williams (1999) and others have used multi-point models.

In this letter we describe the first model for the chemical evolution in a collapsing massive YSO, including the evolution of the central source, infall, and ad/desorption of ices from the grains. The models are used as a clock for studying the evolution of the central source. Here we concentrate on the distri-

bution of H₂O, since it is not only a dominant ice component and important thermal regulator, but also a target of the upcoming Herschel Space Observatory. We apply the model to the AFGL 2591 envelope as it is one of the best observed sources for chemistry in general, and water in particular.

2. Source and Model

AFGL 2591 has been observed in water lines over a range of excitation conditions with both SWAS (Snell et al. 2000) and ISO (Boonman & van Dishoeck 2003). Boonman et al. (2003) used radiative transfer models to constrain the water distribution, with three conclusions: (1) water ice evaporates at $r \sim 10^{16-16.5}$ cm [$T \sim 100$ K in the static model]; (2) $x(\text{H}_2\text{O})_{T>100} \equiv n(\text{H}_2\text{O})/n(\text{H}_2)_{T>100} = 2 \times 10^{-4}$; and (3) $x(\text{H}_2\text{O})_{T<100} \leq 10^{-8}$. This distribution has been confirmed by recent H₂¹⁸O observations by van der Tak et al. (2006).

Van der Tak et al. (2000) constructed spherically-symmetric models of AFGL 2591 and found a best fit density power law $n(r) \propto r^{-m}$ where $m \sim 1$. Since the source evolution models of McKee & Tan (2003) break down for $m = 1$ exactly as the pressure gradient vanishes in this limit, we adopt $m = 1.1$. We take a final stellar mass of $m_{*,f} = 20 M_\odot$. All other inputs are taken from McKee & Tan (2003) for cores. Consistent with $m \sim 1$, we adopt a logotropic collapse velocity field (McLaughlin & Pudritz 1997). While chemical and radiative transfer modeling suggest $m = 1$, we also consider an $m = 1.5$ polytrope.

Figure 1 shows the luminosity evolution, $L(t)$. The results are almost independent of $m_{*,f}$. Given $n(r, t)$ and $L(t)$ we solve for $T(r, t)$. Figure 2 shows $T_{\text{dust}}(r, t)$.

The chemical model is based upon the best-fit model of Doty et al. (2002) for AFGL 2591, using the same gas-phase chemical network, cosmic-ray ionization rate, and initial abundances in the cold cloud exterior. In particular, since $L \sim 0$ at $t = 0$, the input mantle composition places all H₂O and CO on the grain surfaces initially. The CO is quickly liberated –

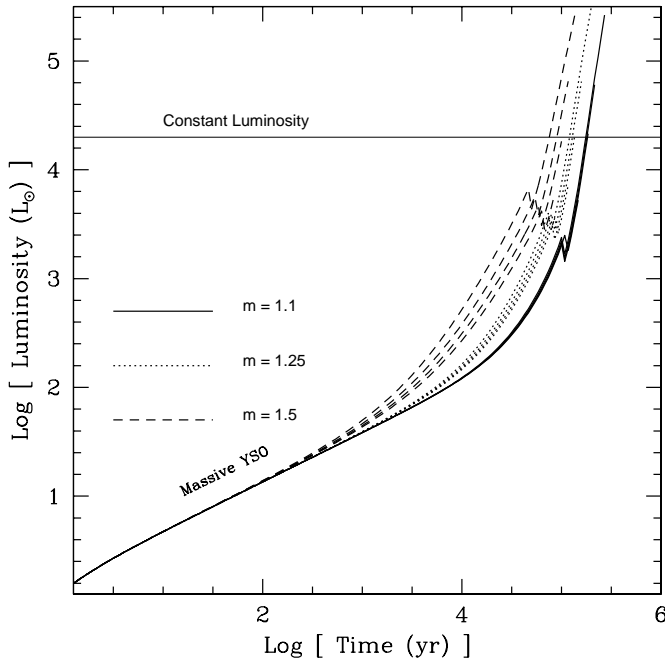


Fig. 1. Evolution of $L(t)$. The curves within each line type correspond to final stellar masses of 40, 20, 12, and 8 M_{\odot} (top to bottom).

by 3×10^3 yr in the H₂O evaporation zone, and by 3×10^4 yr throughout the envelope.

We have made two important modifications. First, we allow the material to infall, solving the chemical evolution in a Lagrangian frame, while simultaneously interpolating on $T(r, t)$. Second we include ad/desorption. For water, we incorporate both the zeroth-order kinetics of Fraser et al. (2001), and the first-order kinetics of Sandford & Allamandola (1988), in turn. For other species, we follow the usual first-order kinetics.

3. Results

The water abundance after including infall and source evolution for $m = 1.1$ is shown in Fig. 3. The abundance constraints are noted by the shaded regions, while the region of the observed evaporation step is noted by the double arrows.

These results can be understood given the fact that for $T_{\text{dust}} > 100$ K, water ice evaporates quickly. As a result, the $T_{\text{dust}} > 100$ K region lies behind an outward propagating evaporation front at which the water ice evaporates nearly instantaneously from the grain surface. The evaporation front stops at $r \sim 3 \times 10^{16}$ cm and $t \sim 2 \times 10^5$ yr, as $m_* \rightarrow m_{*,f}$. For the $m = 1.5$ polytrope, this occurs at $t \sim 9 \times 10^4$ yr.

The water abundance for $T_{\text{dust}} < 100$ K can be understood in terms of ion-molecule chemistry. Here CO is dissociated into O. Proton-transfer processes this into H₃O⁺, which then dissociatively recombines into H₂O. The net result is that CO is gradually transformed into water over time in the cool exterior.

This combination of effects brackets the observational constraints shown in Fig. 3. For $t \leq 3 \times 10^4$ yr, the luminosity has not increased to where the evaporation front can match the observed size of the region of enhanced gas-phase water

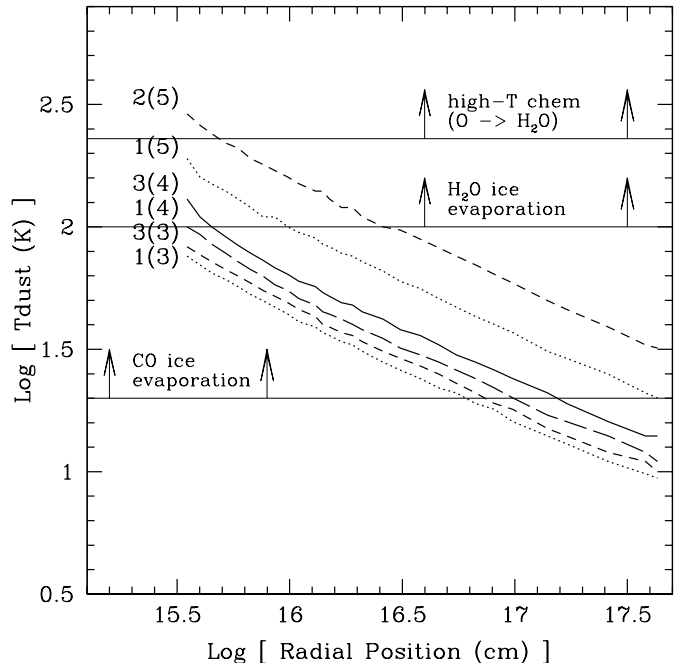


Fig. 2. Temperature distribution as a function of position and time for $m = 1.1$. The curves are labeled by the time in yr.

of $r \sim 10^{16-16.5}$ cm. For $t > 10^5$ yr, the abundance in the outer envelope is too high primarily due to ion-molecule production of water for $T < 100$ K. Together this means that a time $t = 3 - 10 \times 10^4$ yr since YSO formation is sufficient to liberate water, without warming the entire envelope or producing significant ion-molecule chemistry. Results for an $m = 1.5$ polytrope are nearly identical.

Lower stellar masses yield commensurately longer times to reach a given desorption radius, due to their longer Kelvin-Helmholtz timescales. Fig. 1 shows that the observational differences are small: $L(t)$ varies by < 0.5 dex for $8 < m_{*,f}(M_{\odot}) < 40$. Since desorption occurs around $r_{100K} \sim 4 \times 10^{14}$ cm ($L/3L_{\odot}$)^{1/2}, a stellar mass 5 times smaller leads to a desorption radius at any time that is only marginally ($< 1.8\times$) smaller.

To understand other implications, in Fig. 4 we plot the infall trajectories of parcels. Grain mantles quickly evaporate ($T > T_{\text{des}}$) in the shaded region. The lines crossing the trajectories signify where dynamics becomes important ($\tau_{\text{dyn}} \sim t$).

We first note that for parcels originating at $r \leq 10^{16}$ cm, the effects of source evolution dominate collapse, since T reaches T_{des} before dynamics become important. On the other hand, parcels originating at $r > 3 - 6 \times 10^{16}$ cm are dynamic in the mantle evaporation region, due to the fast evolution of the central source. In all cases the gas spends little time above T_{des} .

To see this more clearly, in Fig. 5 we plot the time spent by parcels above T_{des} as a function of their initial position. Qualitatively, the time spent in the warm gas can be understood in three regimes. (I) At early times and small distances, the envelope is \sim static and evolution is dominated by the source. Parcels that begin further out spend more time at high temperatures due to their longer infall distance. (II) An intermediate regime exists where both dynamics and source evolution occur. The shorter times at high temperatures due to the faster

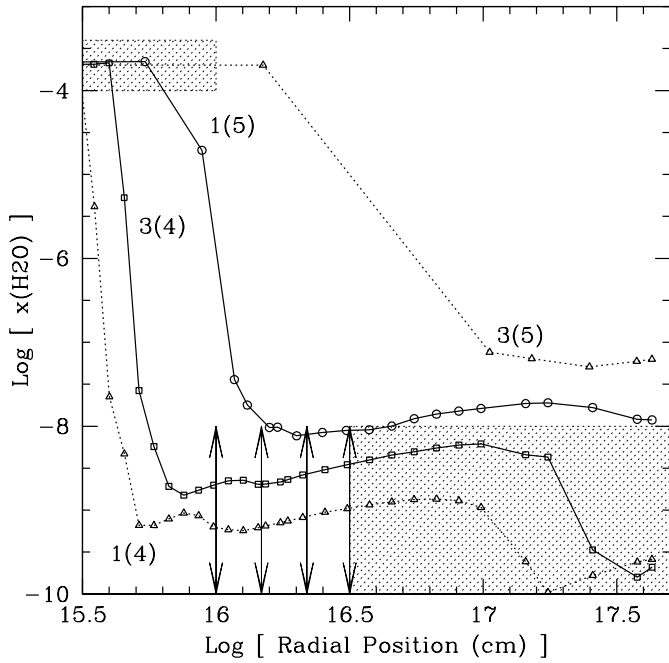


Fig. 3. Water abundance as a function of position in AFGL 2591. The different line types correspond to different times since the formation of the YSO. The shaded areas are the observational constraints.

infall speeds are somewhat balanced by the outward progression of the evaporation front. Finally, (III) cold parcels from far out warm as they fall into the completely evolved inner envelope. In this case, parcels that start progressively further out hit the now stationary evaporation front at progressively higher speeds, leading to less time at high temperatures.

Quantitatively, Fig. 5 shows that parcels spend \sim few \times 10^3 – 10^4 yr as “warm” gas, independent of their starting point. Parcels then enter a region of < 200 AU ($< 0.2''$ at 1 kpc). Such regions are severely beam-diluted and thus nearly invisible. As a result, chemical clocks based upon warm gas-phase (“hot-core”) species – especially observed with single-dish instruments – should show ages of \sim few $\times 10^3$ – 10^4 yr. These ages do not sample the actual age of the source, but instead the residence time in the extended warm gas. The combination of infall, evaporation, and source evolution naturally explains the observed consistency of chemically inferred ages of hot cores between sources.

Since the outer envelope remains “cold” for $\sim 10^5$ yr, we predict a discrepancy between the ages inferred from hot core molecules and from cold gas-phase species. This is consistent with the chemically-inferred ages of ~ 4 – 40×10^3 yr for hot cores, and $> 10^5$ yr for their cold surrounding envelopes (e.g. Hatchell et al. 1998, Millar et al. 1997).

Taken together, we propose the following picture of high-mass envelope evolution: for $t < 10^4$ yr, the majority of the observable envelope is essentially static, and a cold gas-phase chemistry is seen. As the YSO evolves and warms the envelope, a warm gas-phase “hot-core” chemistry is produced. For $t < 1$ – 8×10^4 yr (depending upon polytropic index), a static hot core of size $r \sim 10^{16}$ cm is produced. After this time, the “hot”

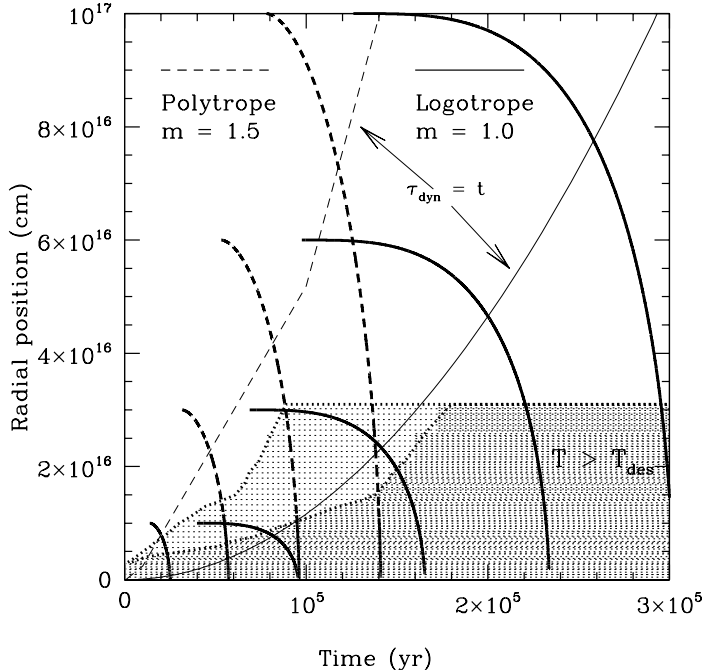


Fig. 4. Infall trajectories of parcels (bold), crossed by lines noting where dynamics become important (thin). The shaded regions signify desorption (dark = logotrope, light = polytrope).

material is dynamic, while much of the cold material remains \sim static. The ice-evaporated hot core chemistry has a characteristic inferred age of \sim few $\times 10^3$ – 10^4 yr, independent of the actual age of the YSO. Finally, once the source reaches the main-sequence, it is hot and luminous enough to ionize the envelope, leading to the disappearance of the hot core after $t \sim 10^5$ yr.

In the scenario above, the infalling material accretes onto a central structure smaller than a few hundred AU. This may be an accretion disk that is diluted in large single-dish observations. Indeed, the disk scale is given by $r_d = 350$ AU $(\beta/0.007)(m_*/20 M_\odot)^{1/2}$, where β is the ratio of rotational to gravitational energy. For high-mass star-formation, $\beta \sim 0.007$ (Pirogov et al. 2003). This size is consistent with a \sim few hundred AU disk inferred by van der Tak et al. (2006) toward AFGL 2591. The column density of this region should be $> 10^{22}$ cm $^{-2}$, suggesting densities $> 10^7$ cm $^{-3}$ and temperatures above 100 K. With lifetimes of 10^5 – 10^6 yr (Cesaroni et al. 2006), this is the regime where warm, complex, second generation chemistry can take place. As a result, future observatories such as eSMA, ALMA, and the EVLA, which can probe scales of $< 0.2''$ will be exquisite tools for uncovering and age-dating the complex circumstellar chemistry.

Lastly, the first-order desorption kinetics of Sandford & Allamandola (1988) yield similar results to the zeroth order kinetics from TPD data. The abundance distributions have the same shape, but shift inward by ~ 0.1 dex in position due to their lower desorption energies. While the order of desorption kinetics is not significant here, it may be important elsewhere.

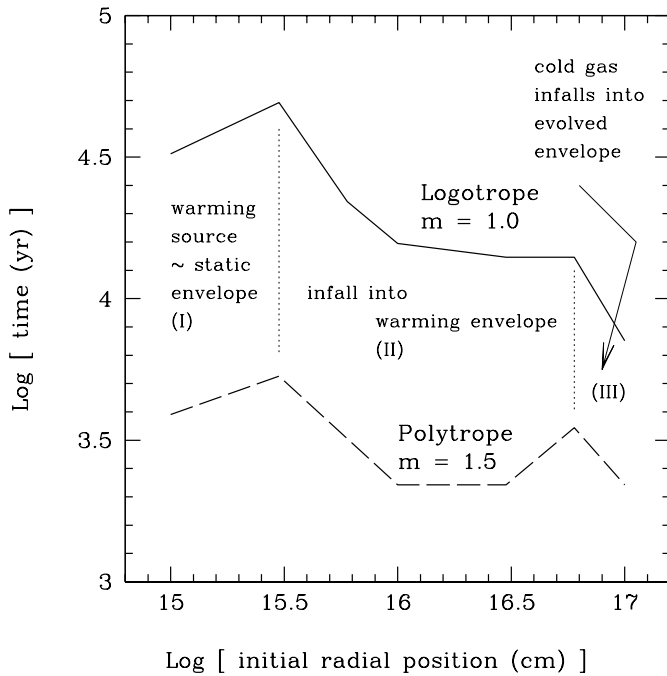


Fig. 5. Time spent above T_{des} in the extended envelope.

4. Conclusions

We have constructed the first model for the chemical evolution in a collapsing massive YSO, including the realistic evolution of the central source as well as the ad/desorption of ices from grain mantles as the grains infall from the cool exterior into the warming interior. This approach allows for a more realistic evaporation of ices from the mantles, as opposed to the more parametric assumptions of previous models. We find that this approach naturally reproduces and explains the parametric step-function water distribution inferred observationally.

The water abundance jump is naturally explained as the propagation of a thermal desorption front outward from the YSO as it evolves. The abundance in the cool outer envelope is explained by ion-molecule reactions which convert CO into H₂O. The time since protostar formation is bracketed by these two processes, yielding an age constraint of $t \sim 8 \pm 4 \times 10^4$ yrs since formation of the YSO. Due to the weak dependence of $T(r)$ on $L(t)$, this timescale should be similar (within 0.5 - 1 dex) for a range of stellar masses.

The combination of the warming envelope and material infall leads to small residence times of material in the warm gas, $\sim \text{few} \times 10^3 - 10^4$ yr, after which the material is beam-diluted in a small structure such as a disk. This naturally explains both the small variance in the ages of hot cores inferred from chemical clocks, as well as the discrepant inferred ages between hot cores and their surrounding halos. Hot cores should disappear in $\sim 10^5$ yr, once the YSO reaches the main sequence and ionizes the envelope. These results suggest that massive star disks should contain most of the complex species on scales of < few hundred AU, which will be observable by the next generation of submm interferometers.

Finally, the order of desorption kinetics assumed (zeroth vs. first-order) are not significant in comparison to source evolution or observational uncertainties.

Acknowledgements. This work was partially supported under grants from The Research Corporation (SDD). Astrochemistry in Leiden is supported by the Netherlands Research School for Astronomy (NOVA) and by a Spinoza and a bezoekersbeurs grant from the Netherlands Organization for Scientific Research (NWO).

References

- Beuther, H., Churchwell, E. B., McKee, C. F., & Tan, J. C. 2006, in Protostars & Planets V, e-print: arXiv:astro-ph/0602012
- Boonman, A. M. S., Doty, S. D., van Dishoeck, E. F., Bergin, E. A., Melnick, G. J., Wright, C. M., & Stark, R. 2003, A&A, 406, 937
- Boonman, A. M. S., & van Dishoeck, E. F. 2003, A&A, 403, 1003
- Caselli, P., Hasegawa, T. I., & Herbst, E. 1993, ApJ, 408, 548
- Cesaroni, R., Galli, D., Lodato, G., Walmsley, C. M., & Zhang, Q. 2006, in Protostars & Planets V, e-print: arXiv:astro-ph/0603093
- Churchwell, E. B. 1999, in The Physics of Star Formation and Early Stellar Evolution II, ed. C. J. Lada, & N. D. Kylafis (Kluwer), 515
- Doty, S. D., van Dishoeck, E. F., van der Tak, F. F. S., & Boonman, A. M. S. 2002, A&A, 389, 446
- Fraser, H. J., Collings, M. P., McCoustra, M. R. S., & Williams, D. A. 2001, MNRAS, 327, 1165
- Lee, J.-E., Bergin, E. A., & Evans, N. J. E. II 2004, ApJ, 617, 360
- Lintott, C. J., Viti, S., Rawlings, J. M. C., Williams, D. A., Hartquist, T. W., Caselli, P., Zinchenko, I., & Myers, P. 2005, ApJ, 620, 795
- McKee, C. F., & Tan, J. C. 2003, ApJ, 585, 850
- McLaughlin, D. E., & Pudritz, R. E. 1997, ApJ, 476, 750
- Hatchell, J., Thompson, M. A., Millar, T. J., & Macdonald, G. H. 1998, A&AS, 133, 29
- Millar, T. J., Macdonald, G. H., & Gibb, A. G. 1997, A&A, 325, 1163
- Nomura, H., & Millar, T. J. 2004, A&A, 414, 409
- Pirogov, L., Zinchenko, I., Caselli, P., Johanson, L. E. B., & Myers, P. C. 2003, A&A, 405, 639
- Rodgers, S. D., & Charnley, S. B. 2003, ApJ, 585, 355
- Sandford, S. A., & Allamandola, L. J. 1988, Icar, 76, 201
- Snell, R. L., Howe, J. E., Ashby, M. L. N., et al. 2000, ApJ, 539, L101
- van der Tak, F. F. S., van Dishoeck, E. F., Evans, N. J. II, & Blake, G. A. 2000, ApJ, 537, 283
- van der Tak, F. F. S., Walmsley, C. M., Herpin, F., & Ceccarelli, C. 2006, A&A, 447, 1011
- Viti, S., Collings, M. P., Dever, J. W., McCoustra, M. R. S., & Williams, D. A. 2004, MNRAS, 354, 1141
- Viti, S., & Williams, D. A. 1999, MNRAS, 305, 755